

## W-Band receiver with Zero Bias Diode operated in the 23K - 295 K temperature range

A.C. Bunea<sup>1</sup>, D. Neculoiu<sup>1,2</sup>, A.M. Avram<sup>1</sup>, and A. Muller<sup>1</sup>

<sup>1</sup>National Institute of R&D in Microtechnologies Bucharest, Romania

Email: alina.bunea@imt.ro

<sup>2</sup>”Politehnica” University of Bucharest, Romania

Email: dan.neculoiu@imt.ro

**Abstract.** In this paper we analyze the influence of extremely low temperatures on the operation performances of a hybrid integrated W-band (75 – 110 GHz) receiver based on a zero-bias GaAs diode. First, the zero-bias diode is investigated and modeled in the temperature range of operation. Then, a direct detection receiver consisting of a membrane supported folded slot antenna and a detection circuit based on a zero-bias diode is fabricated and characterized. The detection circuit is inserted in a cryogenic system and on-wafer measurements are performed in the temperature range 23 K – 295 K, in advanced vacuum conditions. The detection circuit is fed with a 1 kHz amplitude modulated W-band signal and both detected signal and  $i/v$  characteristic are compared for different temperatures. It is demonstrated that the receiver is capable of operating even at 23 K ( $-250.15^{\circ}\text{C}$ ), when the diode is biased at +0.25 V.

**Keywords:** cryogenic; GaAs;  $i/v$  characteristic; receiver; space applications; W-band; zero-bias diode;

### 1 Introduction

Temperatures in space can vary to extremes. For example the blackbody temperature at a distance from the Sun corresponding to the position of Mercury is around  $+180^{\circ}\text{C}$ , while the position of Pluto corresponds to a blackbody temperature of around  $-270^{\circ}\text{C}$  [1]. The operating temperature range of the considered components depends on their position on the spacecraft and on the type of component, as well as on the position of the spacecraft with regard to the Sun. For example the solar panels of a satellite orbiting the Earth operate between  $-100^{\circ}\text{C}$  and  $+125^{\circ}\text{C}$  [2].

As millimeter-wave devices are increasingly being used for space applications [3], considerations such as low-temperature operation must also be taken into account when designing high-performance communication systems.

To extend the receiver front-end applications into cryogenic environments the mechanical and electrical properties of hybrid integrated circuits at cryogenic temperatures should be investigated.

In this paper we analyze the influence of extremely low temperatures on the operation performances of a hybrid integrated W-band receiver based on a zero-bias GaAs diode. On-wafer measurements are performed in a temperature range of 23 K – 295 K. The low-frequency detected signals and the  $i/v$  characteristics are compared at various temperatures.

Since no physical based model is reported in the literature for low temperature range, the exponential law diode model is used to extract the temperature dependence of the corresponding model parameters in the whole temperature range. The model can be used to optimize the performance of the receiver at cryogenic temperature operation.

A W-band (75 – 110 GHz) direct detection receiver consisting of a membrane supported folded slot antenna and a detection circuit based on a zero-bias diode (ZBD) was designed and fabricated. The antenna is processed on a  $2.1 \mu\text{m}$  thick  $\text{SiO}_2/\text{Si}_3\text{N}_4$  ( $1.5/0.6 \mu\text{m}$ ) membrane released through deep reactive ion etching (DRIE) of high-resistivity silicon and the detection circuit is processed on silicon bulk. A photo of two hybrid integrated direct detection receivers, mounted on test PCBs, with SMA connectors for signal extraction are shown in Figure 1.

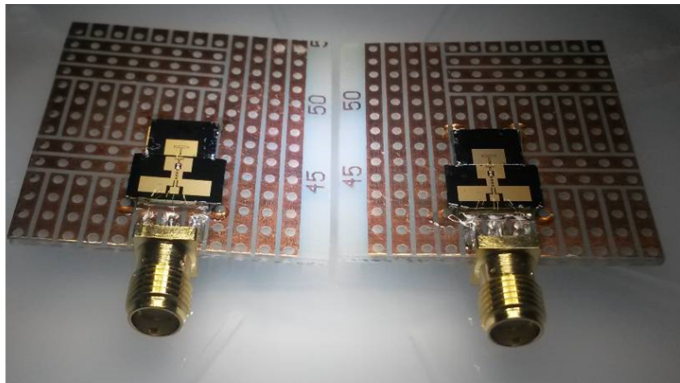


Fig. 1: Photo of two test structures on test PCBs with SMA connectors for the low frequency signal extraction

## 2 Zero-Bias Diode Modeling

The detector diode is the basic building block in the direct detection receiver. Usually, in the millimeter wave frequency range, Schottky diodes are the favorite choice to implement this function. The diode internal resistance at zero bias is very high (in the  $\text{M}\Omega$  - tens  $\text{M}\Omega$  range) and makes the diode matching very difficult, even impossible. In order to achieve good matching, the device needs to be DC biased with a current of several hundred micro-amperes. The internal resistance can be decreased at values of few hundred ohms at the cost of increased noise level and the need of an external bias circuit. To overcome these issues, the GaAs diode structures are designed in such a way that even at zero bias the internal resistance is only few kilo-ohms.

A diode is a two terminal device with nonlinear current/voltage or charge voltage characteristic. In the microwave direct detection (video detection) receivers, the nonlinear  $i/v$  characteristic is used. For the diodes based on a pn junction or on a

Schottky junction the  $i_D/v_D$  characteristic can be modeled with equation (1) with two main parameters  $I_S$  and N. The  $I_S$  parameter is proportional with the device area; the ideality coefficient N takes values between 1 and 2. For a certain range for the bias current/voltage, equation (1) can be used to model the  $i/v$  characteristic of other diodes, even though it is difficult to derive an equation like (1) starting from the structure basic operating principle. In this case the values of the model parameters must be extracted from experimental data and the values for N can exceed 2. The diode model described by (1) must include two physically based components: the series resistance  $R_S$  and the junction parallel capacitance  $C_J$ .

$$i_D = I_S \left[ \exp\left(\frac{qv_D}{NkT}\right) - 1 \right] \quad (1)$$

where  $I_S$  is the diode saturation current; N is the ideality coefficient.

Because of the exponential behavior of (1), it is represented in the semi-logarithmic coordinates as a straight line. Using this representation it is possible to estimate the model parameters  $I_S$  and N using least squares approximation of the straight line region and extracting the slope and the intercept point with the vertical axis. From the slope and the device temperature the N parameter can be computed and from the intercept point the  $I_S$  parameter can be estimated. The effect of the N parameter is illustrated in Figure 2 in forward bias conditions for  $I_S = 1 \mu\text{A}$ . The slope of the characteristic must be traced at in a range where the voltage is higher than  $0.075 \cdot N$  (at room temperature) but lower than the point where  $R_S$  starts to show its influence.

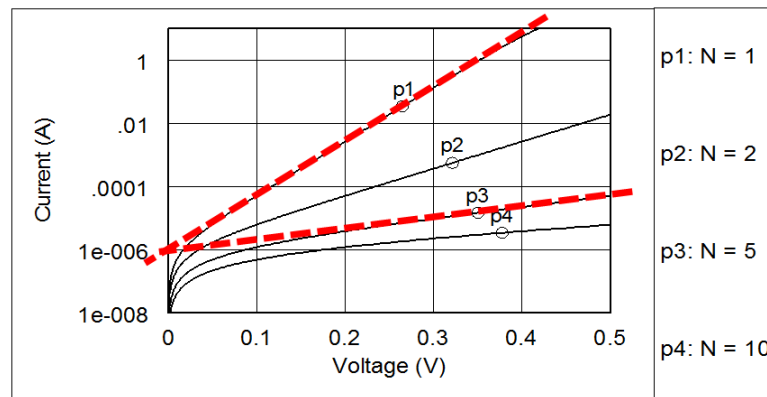


Fig. 2: The diode semi-logarithmic coordinates  $i/v$  characteristic in forward bias conditions with ideality coefficient N as parameter (the method to extract the intercept point with the vertical axis is also illustrated)

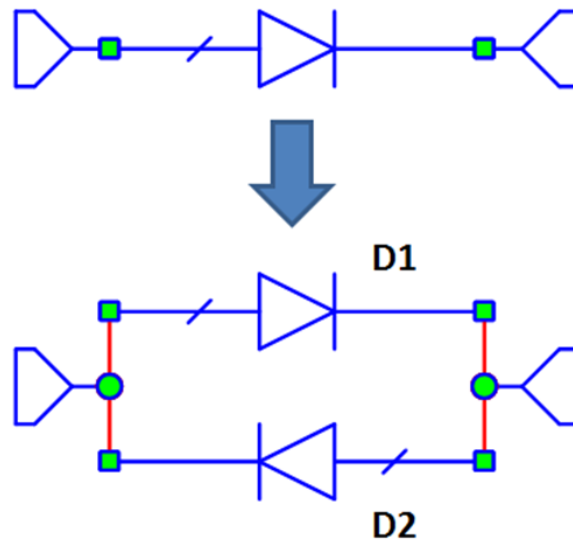


Fig. 3: The ZBD equivalent circuit with two diodes in antiparallel connection

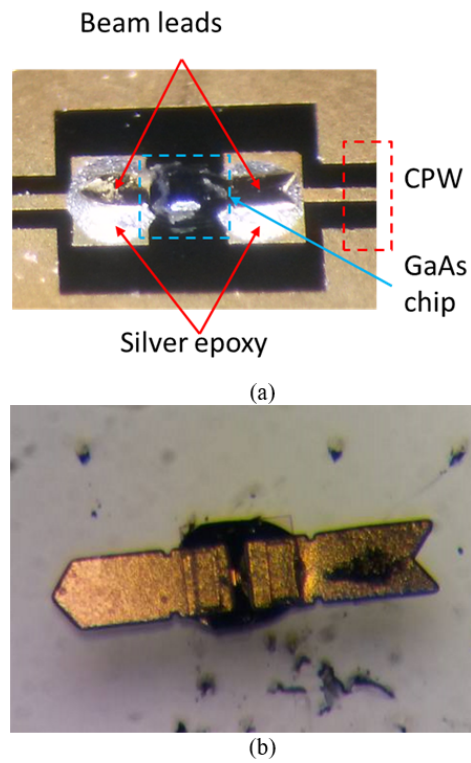


Fig. 4: The beam lead MZBD-9161: a photo of a mounted device (a) and a photo from the back side of the device (b)

The diode was investigated for temperatures between 23 K and 295 K with the experimental setup that will be described in Section 4.

The  $i/v$  characteristics were recorded using a semiconductor characterization system (Keithley 4200 – SCS). At room temperature (295 K), the saturations currents, the ideality coefficients and the series resistances are extracted from the experimental  $i/v$  characteristics and the values are D1 ( $N=1.22$ ;  $I_S = 6.3 \mu\text{A}$ ;  $R_S=31 \Omega$ ) and D2 ( $N=14.9$ ;  $I_S = 5.5 \mu\text{A}$ ;  $R_S=20 \Omega$ ). A comparison between the measured and simulated  $i/v$  characteristics is presented in Figure 5 and the agreement is very good. The characteristic slope at zero bias voltage is about  $3 \text{ k}\Omega$ , in good agreement with the data range provided by the data sheet.

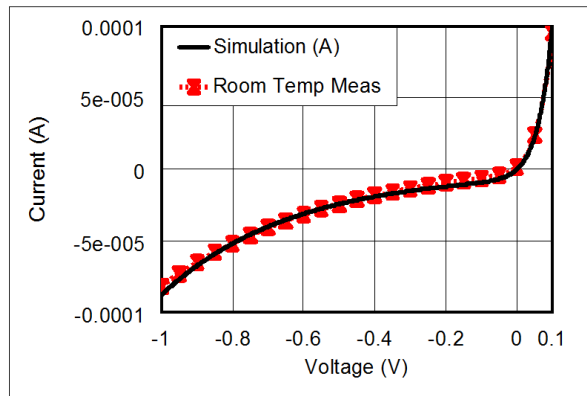


Fig. 5: The  $i/v$  characteristic of the MZBD-9161 at room temperature: simulated (black) and measured (crosses, red)

The  $i/v$  characteristics recorded for temperatures between 295 K and 23 K are shown in Figure 6 (a), for a voltage sweep between  $-4 \dots +1 \text{ V}$ , with a detail of the positive voltages given in Figure 6 (b). The maximum current is limited at  $0.1 \text{ mA}$  to protect the diode.

A shift of the whole  $i/v$  characteristic is noticed with a decrease in temperature. It can be noticed that the slope of the  $i/v$  characteristic in the origin decreases with a decrease in temperature, but the shape of the traces is preserved. This can be translated as an increase of the junction resistance. This leads to the conclusion that the detection properties of the diodes will be preserved at lower temperatures, even if the amplitude of the signal might decrease due to mismatching. The mismatching can be compensated in part by biasing the diode with positive voltages, in order to decrease the diode internal resistance.

From the measured  $i/v$  characteristics, the model parameters for D1 ( $I_{S1}$ ,  $N1$ ) were extracted in forward bias conditions and for D2 ( $I_{S2}$ ,  $N2$ ) in the reverse bias conditions. The method illustrated in Figure 2 was used. No physical based model is reported in the literature for low temperature range, even for a Schottky diode. Moreover, the real layer and doping structure of the ZBD is unknown because it represents an industrial secret. The measurement based investigation of the ZBD model represents the only viable solution for the modeling of the structure in the very low temperature range. The model can be used to optimize the performance of the receiver at cryogenic temperature operation.

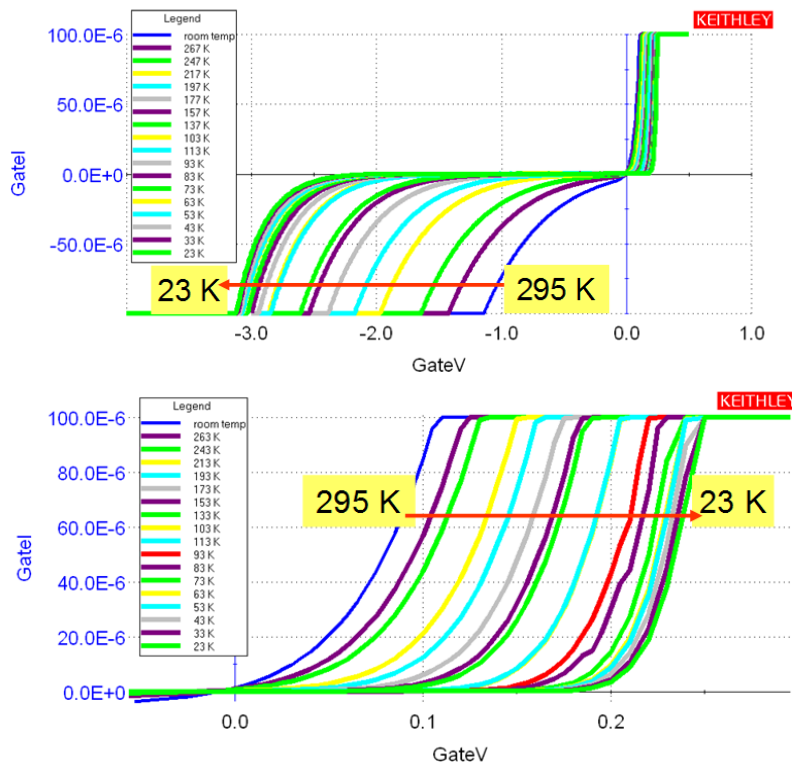


Fig. 6: The i/v characteristics of the MZBD-9161 at temperatures between 295 K (room temperature) and 23 K (linear scale): (a) full scale; (b) detail of positive voltage range

The measured values for the ideality factors are represented in Figure 7 (a) as a function of  $1/T$ . For the diode D1 the ideality coefficient increases from 1.22 at 295 K to 8 at 23 K. For the diode D2 the ideality coefficient increases from 15 at 295 K to 118 at 23 K. The dependence of both ideality coefficients at a temperature smaller than 50 K becomes almost linear with  $1/T$ .

Figure 7 (b) represents the product  $N \cdot T$  as a function of  $1/T$ . The product becomes almost constant at a temperature lower than 50 K.

The measured values for the saturation current as a function of temperature are represented in Figure 8 using semi-logarithmic coordinates. The saturation current has the same order of magnitude and the same shape of the temperature dependence.

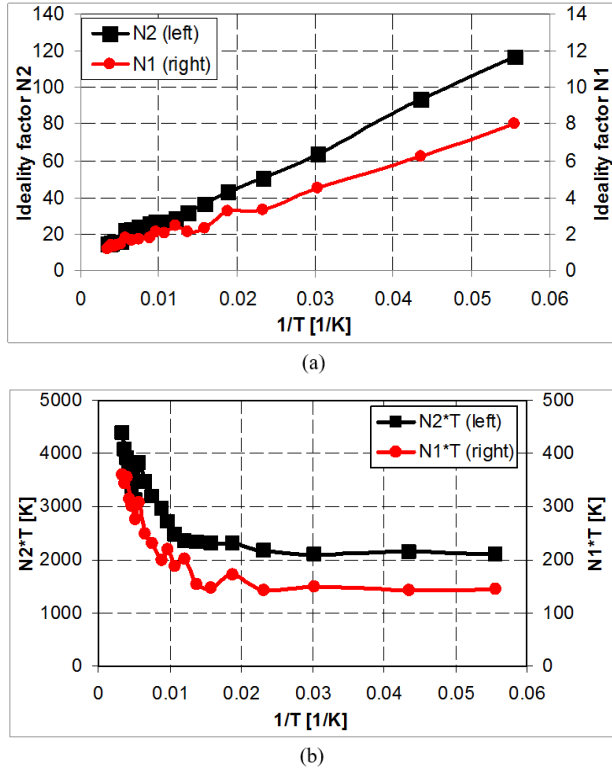


Fig. 7: Ideality factor of the two diodes extracted from measurement results (temperature between 23 – 295 K): (a) as a function of the inverse of the temperature; (b) multiplied by the temperature, as a function of the inverse of the temperature

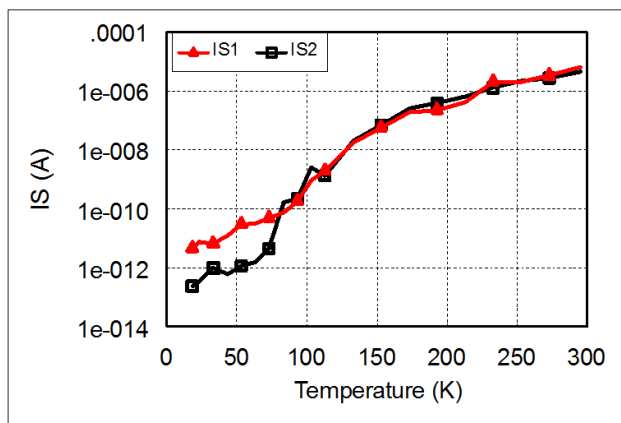


Fig. 8: Saturation current for the two diodes as a function of temperature (23 – 295 K)

### 3 Direct Detection Receiver

The detection circuit consists of a matching network, the diode pads and a low-pass filter [4]. The low-pass filter consists of a cascade of CPW low-impedance/high-impedance sections [5]. The low-Z sections has a characteristic impedance of 24 Ohm, while the high-Z section has a characteristic impedance of 97 Ohm. This filter extracts the DC/low-frequency signal, removes high order spectral components and reflects the W band signal back to the detector diode. The matching network has a stub-line configuration, with a CPW symmetrical shorted stub. The characteristic impedance of the CPW stubs is 35 Ohm.

A 3D electromagnetic model of the detector layout was developed in CST MWS and is shown in Figure 9 (a). The substrate is high-resistivity Silicon, with a thickness of 525  $\mu\text{m}$  and the metallization is 1  $\mu\text{m}$  of gold. The diode was included as a small signal model between the two pads, using the lumped element feature of the simulation software.

The Aeroflex/Metelics MZBD-9161 is a GaAs beam lead detector diode and it is intended for zero bias detecting applications at frequencies up to 110 GHz. The data sheet main electrical specifications for high frequency operation are: junction capacitance  $C_j = 0.035$  pF and video resistance at zero bias  $R_V = 2.5 - 7.5\text{k}\Omega$ . The diode is integrated on the pads using silver epoxy. Figure 9 (b) and (c) show the simulated and the measured  $|S_{11}|$  parameter, respectively, at the port which will be connected to the antenna (input of the matching network).

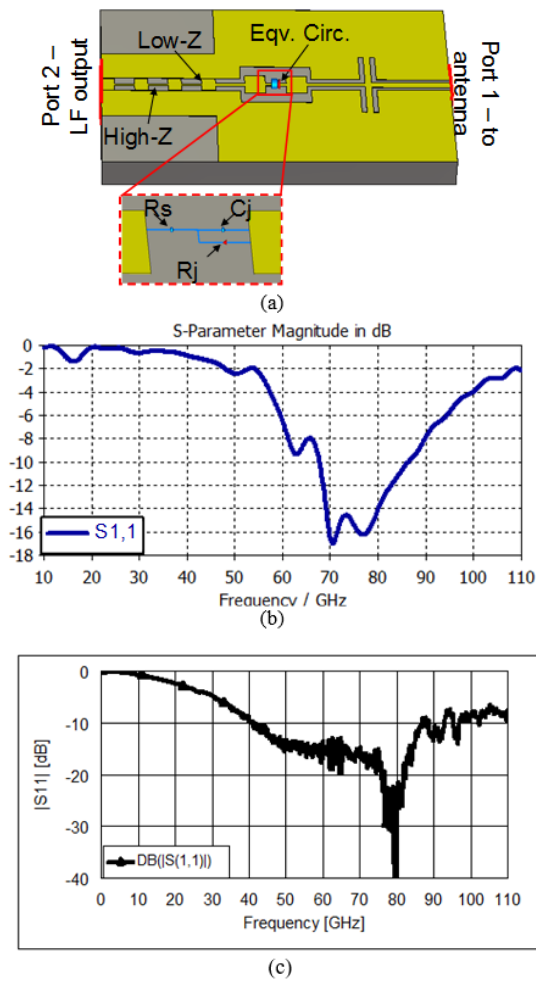


Fig. 9: (a) 3D electromagnetic model of the detector layout; (b) simulated  $|S_{11}|$  parameter at the input of the matching network; (c) measured  $|S_{11}|$  parameter at the input of the matching network

It must be noted that the matching network design provides the DC return path for the diode through the short-circuited stubs. This is necessary even for a "zero bias" diode because the diode nonlinearity will detect the input high frequency signal and generate a very small but nonzero DC component. The DC return path is necessary also to investigate the effect of an external DC bias on the receiver performances.

The detection circuit is connected to the membrane supported antenna by wire-bonding with  $17 \mu\text{m}$  gold wires using the double bonding method in order to decrease the parasitic inductance of the wires. More detailed information about the design of the antenna can be found in [6].

A schematic of the measurement setup for the characterization of the hybrid integrated receiver is shown in Figure 10. It consists of a millimeter-wave source (an Agilent E8257D PSG Analog Signal Generator, with a OML S10MS-AG extension module up to 110 GHz) connected to a standard gain horn antenna, as the emitter.

A millimeter wave signal is modulated with a square wave amplitude modulation (AM) and transmitted towards the receiver. The AM signal is extracted by the detector diode. The detected signal is collected from a support PCB using cables with SMA connectors and displayed on a Tektronix digital phosphor oscilloscope (DPO2024). The amplitude of the detected signal corresponds directly to the received power when the modulation index is 100 (on-off keying).

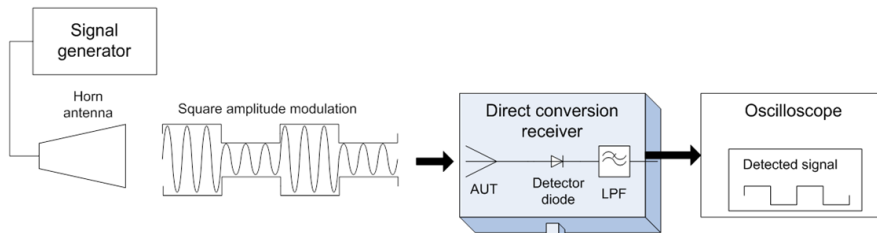


Fig. 10: Schematic of the measurement setup for the characterization of the hybrid integrated receiver

The detected voltage of two samples of hybrid integrated direct detection receivers as a function of frequency, at room temperature and for zero bias conditions, is shown in Figure 11. The maximum detected voltage is around 87 GHz (5.2 mV) indicating that the best matching between the diode and the membrane supported antenna connected with the double gold wire bonding is around this frequency.

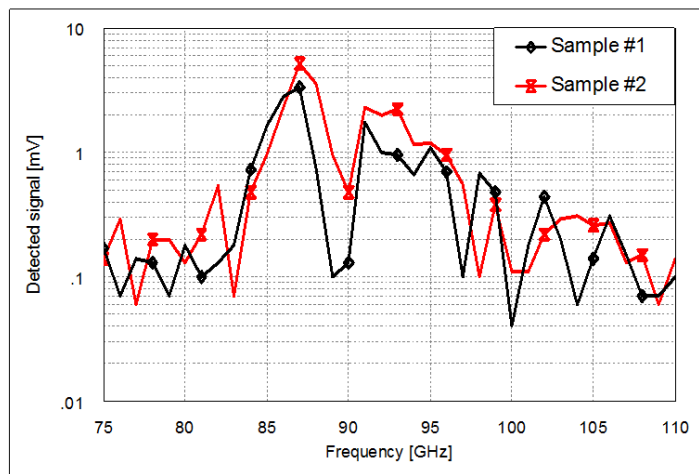


Fig. 11: Hybrid integrated direct detection receiver: detected voltage as a function of frequency at room temperature for two samples

## 4 RF and DC Cryogenic Characterization

In order to get a good estimate of the behavior of the receiver at low temperatures, the detection circuit was placed in a cryostat with an on-wafer measurement setup Figure 12.

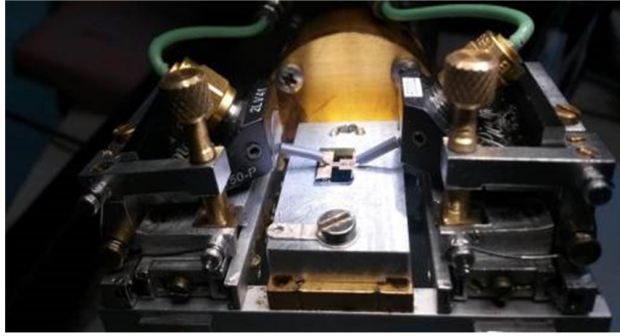


Fig. 12: Photo of the device under test in the cryogenic on-wafer measurement setup

This setup allows for testing both in DC as well as in microwave and uses standard G-S-G probes (Picoprobe) with a pitch of 150 microns to contact the circuit. The target of this experiment is related to space applications, where the system should be able to operate in extremely low temperature conditions.

The schematic of the measurement setup is shown in Figure 13. The W-band signal generator is a synthesized source Agilent PSG E8557D with a OML W-band module. It provides a 1 kHz rectangular amplitude modulated (AM) signal, which is applied at the coplanar waveguide (CPW) input of the detection circuit, placed in the cryostat.

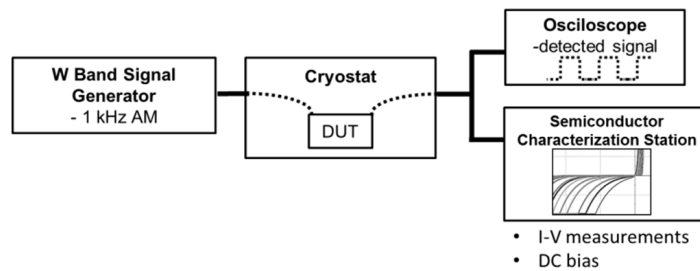


Fig. 13: Schematic of the cryogenic measurement setup

The signal is then demodulated by the diode, filtered by the low-pass filter (LFP) and picked-up by the second CPW probe, placed at the output of the LPF, the signal is then displayed on a digital oscilloscope that gives the amplitude of the detected signal. This characterization technique was intensely used in [4] and [7] - [9] for the characterization of direct conversion (video) receivers.

A semiconductor characterization system (SCS Keithley 4200) is also connected to the second (output) probe, enabling the recording of  $i/v$  characteristic at different temperatures. The SCS can also be used to bias the detector diode, if needed.

Figure 14 shows the  $i/v$  characteristics and the detected signal at 295 K (Figure 14

(a) and (b), respectively) and at 23 K (Figure 14 (c) and (d), respectively) for a 94 GHz carrier frequency. It is remarkable that even at such a low temperature the device still operates.

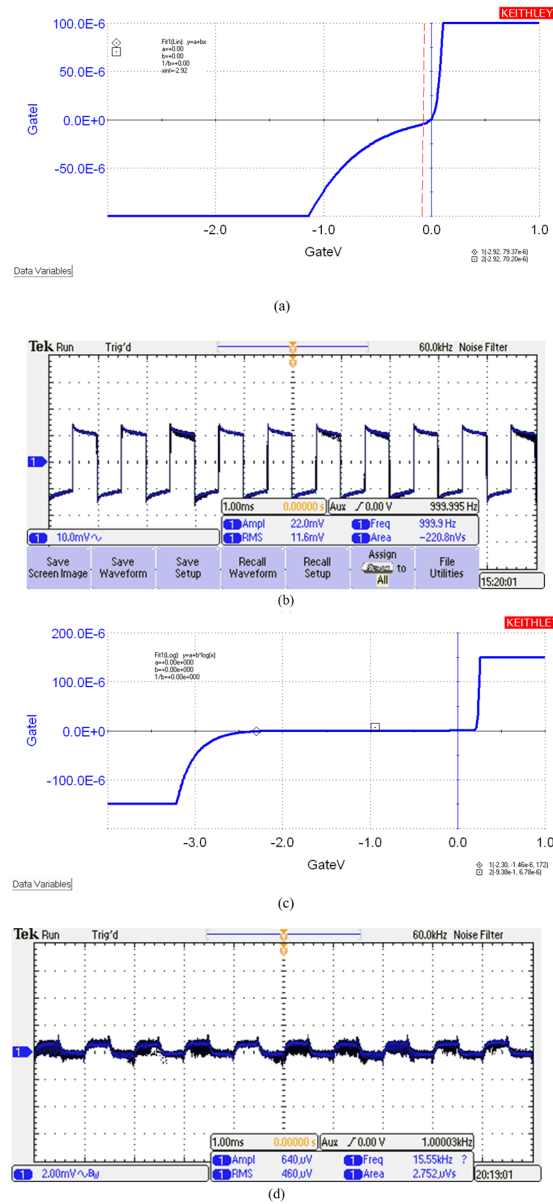


Fig. 14: Measurement results: (a) i/v characteristic at 295 K; (b) detected signal at 295 K; (c) i/v characteristic at 23 K; (d) detected signal at 23 K

At a temperature of 23 K, the diode had to be biased with a voltage of +0.25 V. The negative voltage over the diode drops by approx. 2.1 V, for a 0.1 mA reverse current, resulting in a voltage drop with temperature of 7.6 mV/K.

## 5 Conclusion

A hybrid integrated W-band direct detection receiver based on a zero-bias GaAs detector diode was presented. The receiver consisted of a single folded slot antenna, processed on a thin dielectric membrane connected with bond-wires to a detection circuit comprised of a set of matching stubs, rectangular diode pads, low-pass filter and low-frequency output. The GaAs diode was hybrid-integrated in the detection circuit using silver epoxy. The zero-bias diode was modeled with the exponential law and the ideality factors and saturation currents values were extracted for the whole temperature range. Cryogenic experiments in advanced vacuum conditions were performed on the detection circuit and the results showed the viability of the proposed receiver for low temperature operation.

**Acknowledgements.** This work was supported by the Romanian Ministry of Research and Innovation, under the project no. PN-II-ID-PCE-2011-3-0830 and project no. PN-III-P2-2.1-PED-2016-0976, as well as by the Romanian Space Agency (M3GAAS STAR Contract CF86/2013).

## References

- [1] DAVID G. GILMORE, *Spacecraft Thermal Control Handbook*, Volume 1 - Fundamental Technologies (2nd Edition), American Institute of Aeronautics and Astronautics/Aerospace Press, 2002
- [2] VINCENT L. PISACANE, *Fundamentals of Space Systems*, New York: Oxford University Press, 2005.
- [3] J. MOLL, M. KOTIRANTA, B. HILS AND V. KROZER, "A 100 GHz millimeter wave radar system with 32 transmitters and 32 receivers for space applications," Radar Conference (EuRAD), 2012 9th European, Amsterdam, 2012, pp. 361-364.
- [4] ALINA-CRISTINA BUNEA, DAN NECULOIU, PIERRE CALMON, ALEXANDRU TAKACS, "Design and Characterization of a Micromachined Receiver for W Band Applications", IEEE EuMW 2014, Rome, Italy, 5-10 October 2014, pp. 937-940
- [5] EDWARDS T. C. , STEER M. B. , "Foundations of Interconnect and Microstrip Design", 3rd Edition, J. Wiley & Sons, 2000
- [6] A. C. BUNEA, DAN NECULOIU, ANDREI AVRAM, "Design and Analysis of a Membrane Supported Folded Slot Antenna for W-Band Applications" , UPB Scientific Bulletin: Series C: Electrical Engineering and Computer Science, pp. 109-120, vol. 78, Iss.2, 2016
- [7] D. NECULOIU, A-C. BUNEA, A. MULLER, "Ground Speed Doppler Sensor with a Micromachined Double Folded Slot Antenna", Proceedings of the IEEE Asia-Pacific Microwave Conference, APMC-2015, Nanjing, China, 6-9 December 2015, vol. 3,
- [8] ALINA-CRISTINA BUNEA, DAN NECULOIU, MARKKU LAHTI, TAUNO VAHAHEIKKILA, "LTCC Microstrip Parasitic Patch Antenna for 77 GHz Automotive Applications", IEEE Conference on Microwaves, Communications, Antennas and Electronic Systems IEEE COMCAS 2013, Tel Aviv, Israel, 21-23 October 2013
- [9] BUNEA A.C. ,NECULOIU D., AVRAM A.M., MLLER A., "Hybrid integrated direct detection receiver for W-Band space applications operated in cryogenic conditions", IEEE 39th International Semiconductor Conference IEEE CAS 2016, Sinaia, Romania, 10-12 October 2016, pp. 67-70